Erschienen in: Solar Energy Materials and Solar Cells ; 72 (2002), 1-4. - S. 155-163
https://dx.doi.org/10.1016/S0927-0248(01)00160-X

Comparing improved state-of-the-art to former EFG Si-ribbons with respect to solar cell processing and hydrogen passivation

P. Geiger*, G. Hahn, P. Fath, E. Bucher

Universität Konstanz, Fachbereich Physik, Fach X916, 78457 Konstanz, Germany

Abstract

Recently, the ASE Company succeeded in enhancing the material quality of their octagon edge-defined film-fed growth (EFG) silicon ribbons resulting in a higher average cell efficiency in the manufacturing line of ASE Americas. In order to quantify and characterize these improvements in material quality, lifetime measurements have been performed on state-of-the-art and, for comparison reasons, also on older EFG material. Moreover, these wafers were subjected to a laboratory solar cell process. Consequently, it has been possible to perform laser beam induced current (LBIC) mappings and to compare the resulting internal quantum efficiency (IQE) mappings to the lifetime measurements performed before cell processing. As a result we found typical, different distributions of lifetime and IQE for the two materials. Further on, the solar cells have been hydrogen passivated using a microwave-induced hydrogen plasma and characterized again so that the impact of this passivation technique on the materials in different states of development could have been investigated. In this way, an appropriate hydrogen defect passivation turned out to reduce the differences between the different kinds of EFG ribbons.

Keywords: EFG; Lifetime mapping; LBIC mapping; Hydrogen passivation

1. Introduction

For large-scale applications of photovoltaic modules, there is still a need for cost decrease. Octagon edge-defined film-fed growth (EFG) silicon supplied by ASE is a promising candidate to reach this goal. The multi-crystalline wafers are grown directly out of the melt in the required thickness so that expensive sawing steps and

*Corresponding author. Tel.: +49-7531-88-2132; fax: +49-7531-88-3895.
E-mail address: patric.geiger@uni-konstanz.de (P. Geiger).

related material losses are avoided. According to the specific growth process, however, a certain amount of defects and impurities can be found in the material. Apart from the development of material specific solar cell processing technologies it is therefore necessary to reduce the amount of defects incorporated in the wafers in order to reach higher cell efficiencies.

Recently, ASE Inc. managed to improve the average solar cell efficiency of 10×10 cm^2 EFG wafers from 13.4% to 14.4%. They achieved these results by some cell process alterations and by modifications of the crystal growth procedure like improved purification of graphite used during crystal growth and enhanced control over the uniformity of thickness [1].

To know more about the consequences of changed crystal growth parameters on the material properties might facilitate further improvements of EFG ribbons. For that reason, we have performed lifetime measurements on these new (state-of-the-art) and old EFG wafers in order to gain insight into their differences. Using the same wafers we have processed solar cells so that it has been possible to compare cell parameters and, with the help of laser beam induced current (LBIC) mappings, relate their performance after cell processing to preceding lifetime measurements. Finally, the specific impact of microwave-induced remote hydrogen plasma (MIRHP) passivation [2,3] on the different octagon ribbons has been examined.

2. Lifetime measurements

In order to get a first impression of the properties of the different octagon EFG materials, we have performed spatially resolved minority charge carrier lifetime measurements on various new and old 10×10 cm^2 wafers with passivated surfaces. For that purpose, we made use of the mapping technique of microwave-detected photoconductance decay (PCD) under low injection conditions. Initial measurements had shown very strong variations in lifetimes within one wafer, especially in the case of new EFG material. This causes problems as the PCD technique requires the choice of an adequate time range within which the transient recorder evaluates the PCD, and this time range depends on the magnitude of lifetime values. Consequently, the whole wafer or large areas with a wide distribution of lifetimes cannot be measured properly with one single mapping. For that reason several mappings of the same wafer with different time ranges have been performed and afterwards combined. Typical results for each of the materials are given in Fig. 1. Apart from the stripe-like structure typical for octagon EFG, one can find a higher average lifetime within the state-of-the-art material. This can also be seen in the frequency distributions shown in Fig. 2. The curves of both materials peak at about the same lifetime value of $\tau = 0.7\,\mu$s. In the case of new EFG, however, the distribution is much more shallow and wider as for the old material which seems to be a typical difference between the two different states of development. While in the mapping of the old wafer, one can only hardly find areas with τ-values higher than 2 μs, regions of much higher lifetime have been identified in the new ribbons.

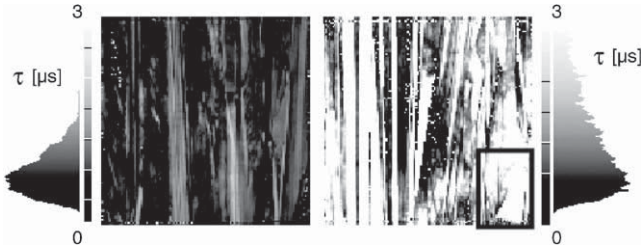

Fig. 1. Typical lifetime mappings of old (left) and new (right) as-grown EFG octagon wafers with passivated surfaces. The marked rectangle is shown in Fig. 3.

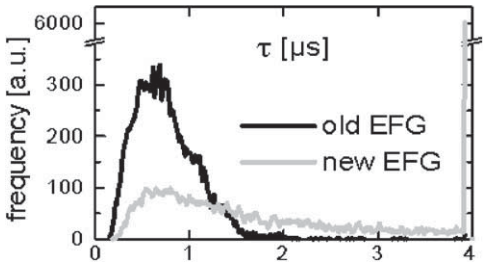

Fig. 2. Frequency distributions of lifetime mappings given in Fig. 1.

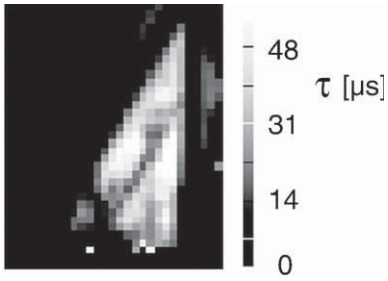

Fig. 3. Enlarged view of the region marked in Fig. 1.

Sometimes even values above 40 μs have been found as visible in Fig. 3 which shows a different scaling of the marked region in Fig. 1.

3. Solar cell processing

For further investigations of the different materials with respect to photovoltaic applications, we have made solar cells out of the different materials. Both kinds of wafers have been processed simultaneously using the laboratory processing sequence that is schematically illustrated in Fig. 4. Apart from an acid defect etching step,

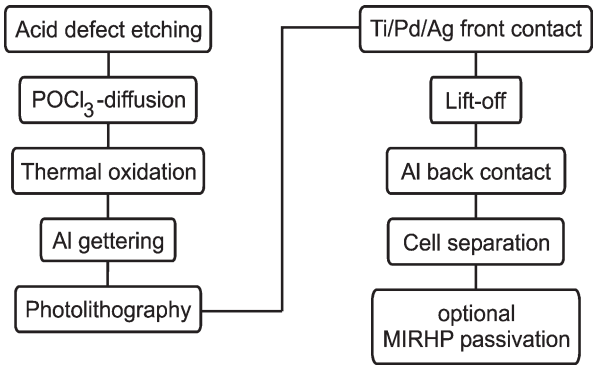

Fig. 4. Processing sequence used for the fabrication of solar cells.

phosphorous diffusion, thermal oxidation and Al-gettering, it covers a photolithographically defined front grid as well as evaporated front and back contacts. Cell separation was realized using a conventional dicing saw so that cells with an area of 2×2 cm^2 have been obtained. At the end, an optional MIRHP passivation step can be applied in order to investigate the impact of hydrogen incorporation on the solar cells made out of different ribbons.

4. Correlation between starting lifetimes and solar cell performance

4.1. LBIC and IQE mappings

LBIC mappings as well as spatially resolved reflectivity measurements have been performed on the processed solar cells. In this way, it is possible to calculate the internal quantum efficiency (IQE) for each point of measurement. Consequently, the solar cell performance can be compared to the starting lifetime in a spatially resolved way.

This has been done for several solar cells made out of old or new EFG using a laser wavelength of $\lambda = 905$ nm. The results for an old one are given in Fig. 5. As expected, the same structures of regions of good and poor performance can be found in the lifetime mapping as well as in the IQE measurement before MIRHP passivation. After hydrogen incorporation, the difference between quite good and rather poor performance is less distinctive but still visible. Consequently, the histogram corresponding to the IQE mapping after passivation is shifted to higher values and has become more narrow.

Solar cells made out of new EFG ribbons have been investigated in the same way. The obtained mappings of one solar cell are given in Fig. 6. This time, the region of interest is marked with a black square in the clipping of the lifetime measurement. For clarification, it stretches beyond the mapping. Again the same structures of good

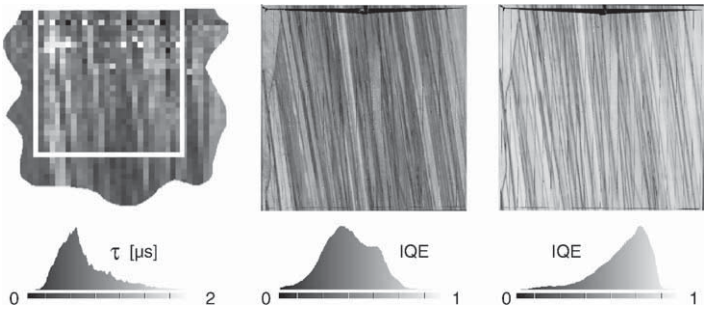

Fig. 5. Clipping of τ-measurement of old EFG wafer (left, white square marks — area of interest), IQE (905 nm) of corresponding solar cell (middle) and IQE (905 nm) of the same cell after 110 min of MIRHP passivation at 275°C.

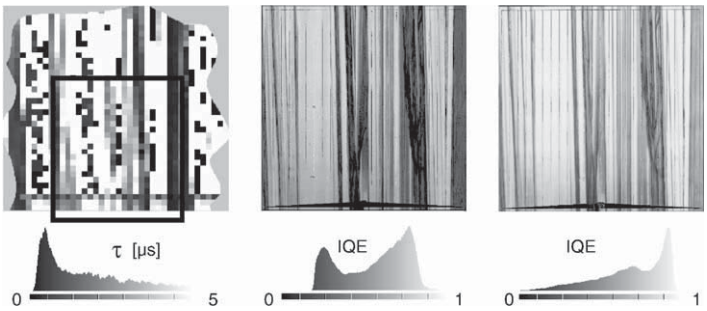

Fig. 6. Clipping of τ-measurement of state-of-the-art EFG wafer (left, black square marks—area of interest), IQE (905 nm) of corresponding solar cell (middle) and IQE (905 nm) of the same cell after 110 min of MIRHP passivation at 275°C.

and bad areas are visible in τ- and IQE-mappings. But a comparison of the IQE measurements before hydrogen passivation shown in Fig. 6 with those given in Fig. 5 reveals higher IQE values within the solar cell made out of new material as compared to the cell made out of old ribbon. Moreover, the mapping in the middle of Fig. 6 shows a double peak structure in the histogram that has been found in all IQE-mappings of new EFG solar cells so far. This special shape of the histogram comes into existance because there are closely neighboured regions of strongly differing performance in the new material. During hydrogen incorporation, however, the very good regions improve less than the rest of the solar cell. This causes the double peak shape to vanish and results in a more narrow distribution of IQE.

4.2. Statistical evaluation of processed solar cells

Solar cells have been processed out of both EFG octagon materials in the way described in Section 3. In order to maintain the comparability of the different silicon materials and related solar cells, it was necessary to process all the wafers within the

Table 1
Mean values and deviations of I–V-characteristics for old and new EFG material, before hydrogen passivation, no antireflection coating

	Old EFG material				New EFG material			
	V_{OC} (mV)	J_{SC} (mA cm^{-2})	FF (%)	η (%)	V_{OC}	J_{SC}	FF	η
Mean value	518	18.4	74.9	7.2	520	19.2	74.4	7.4
Standard dev.	11.0	0.92	0.80	0.55	14.8	1.59	0.63	0.84
Standard err.	2.6	0.22	0.19	0.13	3.0	0.32	0.13	0.17

same process. Therefore, according to limited processing capacities, the statistical evaluation relies on quite small numbers of 18 cells made out of old and 25 made out of new material. That is not enough for a quantitative exploration of data, especially in conjunction with the strong variation of material quality within one wafer. Nevertheless, it should give some principle information about the reaction of the different octagon materials on the applied solar cell process.

Throwing a glance at mean values of the I–V-characteristics before hydrogenation given in Table 1 one finds comparable open circuit voltages V_{OC} for both materials. Mean values of short circuit current density J_{SC} and efficiency η, however, tend to be higher in solar cells made out of state-of-the-art EFG ribbons, whereas the mean fill factor FF is lower. A comparison of standard deviations of the cell parameters shows that, apart from FF, mean values of the new material vary more strongly than those of the older ribbons. This coincides with the results of lifetime measurements presented in Section 2. Frequency distributions of η and J_{SC} given in Fig. 7 show a peak value for old material at comparable low values whereas the distributions of the newer ribbons reach higher values and appear to be wider. However, these graphs might look different for distributions based on $10 \times 10\,\text{cm}^2$ solar cells as the processed ones with an area of 4 cm^2 might be entirely or at least mainly located in an area of quite good or rather poor performance.

5. MIRHP passivation effectiveness

Significant enhancements of solar cell parameters can be achieved by incorporation of atomic hydrogen in silicon containing defects [2]. Therefore, we have investigated the impact of various passivation times at 275°C and 350°C on solar cells made out of old and new EFG silicon. For that purpose, we made use of a MIRHP.

In this way, improvements in efficiency of above 35% relative have been reached in old as well as in new EFG ribbons and with both passivation temperatures (see Fig. 8). Additionally, the absolute efficiencies measured after hydrogen passivation are about the same. Sufficient defect passivation could have been reached after about 20 min of plasma passivation at 350°C or 60 min at 275°C. But apart from required

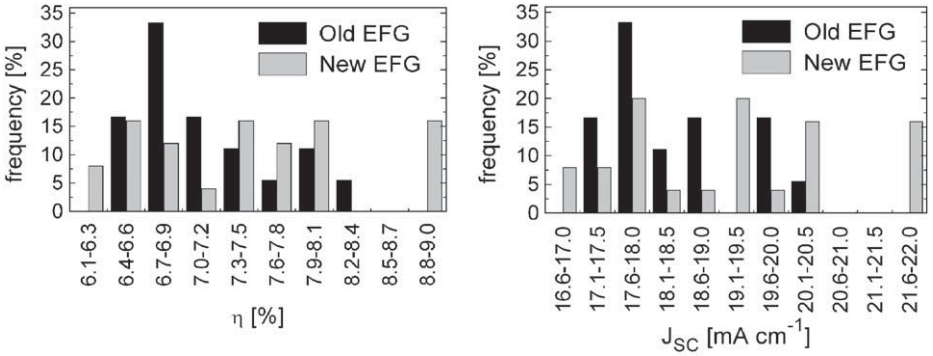

Fig. 7. Frequency distributions of efficiency and short circuit current achieved after cell processing.

time of hydrogen incorporation, passivation temperature seems to be quite uncritical for both materials.

Having a closer look at the efficiency gains in new EFG material achieved by passivation at 350°C, one might find some remarkable differences. As can be seen in Fig. 8, solar cell no. 10 has improved by 40% (rel.) and no. 9 by 34% (rel.). No. 8 only shows an increase in efficiency of 22% (rel.). As, before hydrogen treatment, no. 10 had shown an efficiency 0.7% absolute lower than no. 8, the difference in efficiency improvement between these two cells might be explained by a larger number of defects within no. 10 which could have been passivated by the use of atomic hydrogen afterwards. No. 8, instead, contains less defects so that it has gained less profit by MIRHP passivation but shows a similar final efficiency. According to that, no. 9 which had shown by far the least starting efficiency, should have gained the largest profit by hydrogen passivation. This prediction turns out to be wrong as can be seen in Fig. 8. Consequently, it seems as if there exists an effect that, under certain circumstances, limits the amount of hydrogen that can be incorporated in the solar cell. Another possibility might be an inhomogeneous distribution of different kinds of defects in the material which cannot be MIRHP passivated to the same extent with the used experimental setup. Further investigations will be necessary to answer these questions.

The best solar cell that has been processed within this investigations was passivated for 90 min at 275°C. In this way, an efficiency of 10% without any antireflection coating and a reflectivity of 34% at 905 nm could have been reached ($J_{SC} = 23.0$ mA cm^{-2}, $V_{OC} = 560$ mV, FF = 77.6%).

6. Summary

Wider lifetime distributions extending to higher values have been found to be typical for state-of-the-art EFG octagon material as compared to older EFG

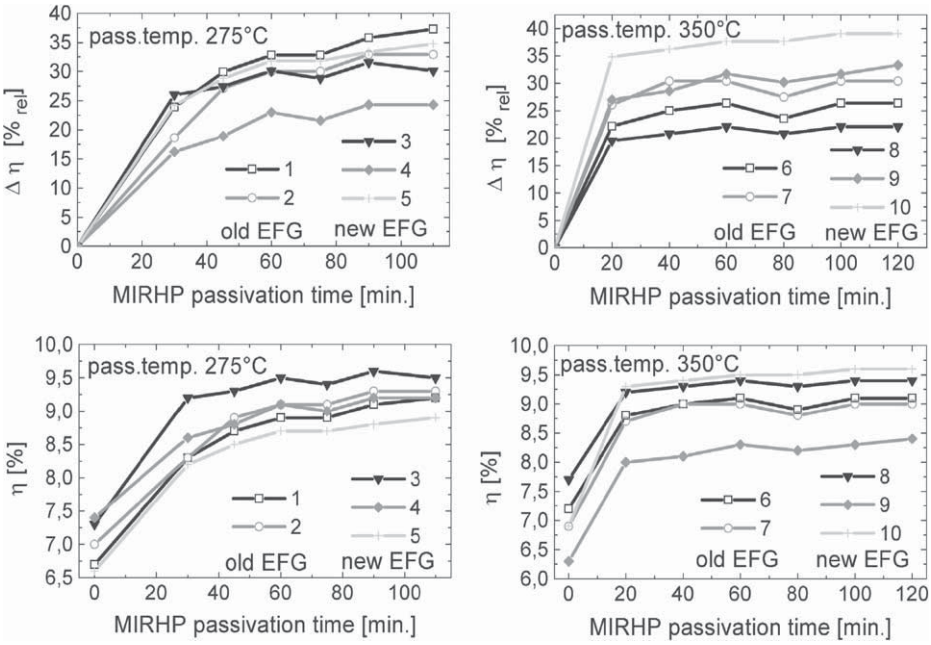

Fig. 8. Relative and absolute efficiency gains in old and new EFG silicon after various hydrogen passivation times at 275°C (left) and 350°C (right).

ribbons. Lifetimes above 45 μs have been measured in the new as-grown material. Nevertheless, there are also regions of rather low lifetime. This leads to a characteristic double peak structure of IQE histograms belonging to laboratory type solar cells processed out of new ribbons. After MIRHP passivation, this twofold peak shape vanishes as defect passivation in regions with rather low starting lifetime has a greater impact on related IQE values than the passivation of remaining defects in areas that had already shown a good starting performance. In agreement with lifetime measurements, a rudimentary statistical evaluation of processed solar cells (4 cm^2) shows extensions of efficiency and short circuit current density distributions for new EFG material to higher values leading to better mean cell parameters with larger deviations for this cell size. MIRHP passivation investigations have revealed both materials to be not very sensitive to passivation temperature with respect to passivation effectiveness but according to the time necessary for sufficient hydrogen incorporation. It has been found that a good defect passivation can be reached after 20 min of hydrogen incorporation at 350°C or after about 60 min at 275°C. Within these investigations, an efficiency of 10% without any reflection coating has been reached. Moreover, some questions according to passivation effectiveness within new EFG material have risen that will have to be addressed in future investigations.

Acknowledgements

This work was supported within the KoSi programme by the German Bundesministerium für Wirtschaft (BMWi) under contract number 0329858J. The technical assistance of M. Keil during cell processing is also gratefully acknowledged.

References

[1] B. Bathey, J. Kalejs, M. Rosenblum, M. Kardauskas, R. Giandcola, J. Cao, in: Proceedings of the 28th IEEE PVSC, Anchorage, 2000, p. 194.
[2] M. Spiegel, S. Keller, P. Fath, G. Willeke, E. Bucher, in: H.A. Ossenbrink, P. Helm, H. Ehmann, eds., Proceedings of the 14th EC PVSEC, Barcelona, 1997, p. 743.
[3] M. Spiegel, P. Fath, K. Peter, B. Buck, G. Willeke, E. Bucher, in: W. Freiesleben, W. Palz, H.A. Ossenbrink, P. Helm, eds., Proceedings of the 13th EC PVSEC, Nice, 1995, p. 421.